31st Annual International Conference of the IEEE EMBS
Minneapolis, Minnesota, USA, September 2-6, 2009

Radar Cross Section of Human Cardiopulmonary Activity for Recumbent Subject

John E. Kiriazi, *Student Member, IEEE*, Olga Boric-Lubecke, *Senior Member, IEEE*, and Victor M. Lubecke, *Senior Member, IEEE*

***Abstract*—The radar cross section (RCS) corresponding to human cardio-respiratory motion is measured for a subject in two different recumbent positions. Lying face-up (supine), the subject showed an RCS of 0.326 m^2. But when lying face-down (prone), the RCS increased to 2.9 m^2. This is the first reported RCS measurement corresponding to human cardio-respiratory motion. The results obtained in this experiment suggest modeling the upper part of the human body as a half-cylinder where the front body corresponds to the cylindrical surface and the back corresponds to the rectangular one.**

I. Introduction

DOPPLER radar shows high potential for monitoring the cardiopulmonary behavior of remote human subjects [1]-[3]. Robust sensing of heartbeat and respiration rates is attractive for many applications such as healthcare, military and security. Much work has been done to accurately measure heartbeat and respiration rates [4]-[5]. However, distinguishing characteristics beyond presence and rates remains a challenge. While the Doppler-modulated phase is proportional to chest movement, the power of the received signal is dependent on the interaction of the wave with the subject's body. The Doppler radar cross section (RCS) is a measure of the magnitude of the wave backscattered off the moving parts of the subject's body. It is dependent on the physical area of the chest as well as the surface reflectivity and directivity at the operating frequency. For human cardiopulmonary motion it is also factor of the chest orientation with respect to the line of sight between the subject and the transceiver. This is due to the asymmetry of the body around the vertical axis and the motion type at each side of the chest.

Previous studies of human radar cross section were either for a man swinging on a platform [6] or for Body of Revolution models [7]. This paper presents the first reported RCS measurement for human cardio-respiratory motion. Understanding the radar cross section due to subject's cardiopulmonary motion is key to enabling accurate interpretation of radar signals in human monitoring, particularly for the assessment of position and depth of cardiopulmonary motion. In this paper, theory and experiments describe the radar cross section associated with respiration and heartbeat, and its dependence on subject orientation. A radar system using a homodyne quadrature receiver with dc coupling and arctangent demodulation [8] was developed to accurately capture the necessary details for RCS analysis.

Manuscript received June 20, 2009. This work was supported in part by the NSF under grants ECS0428975 and ECS0702234.

J. E. Kiriazi, O. Boric-Lubecke, and V. M. Lubecke are with the Department of Electrical Engineering, University of Hawaii at Manoa, Honolulu, HI 96822 USA (phone: 808-956-9776; e-mail: kiriazi@hawaii.edu).

II. Quadrature Doppler Radar

The cardiopulmonary activity of a human subject is manifested in the chest movement. The Doppler radar motion sensor typically uses a continuous wave illuminating the subject. The reflected wave backscattered off the subject's torso is phase modulated by the torso movement due to the Doppler effect. By comparing the phase of the reflected wave with the transmitted one, a baseband signal proportional to the displacement in the line of sight is obtained. In quadrature receiver configuration, shown in Fig. 1, the baseband signal is obtained from the two orthonormal components, namely the I-channel and Q-channel. Each channel is filtered, amplified and digitally acquired independently. The digital signal processing stage then applies the optimum demodulation technique, in this case, the center estimation algorithm [9]. This configuration avoids having the phase demodulation accuracy highly fluctuating with distance, bouncing between null and optimum points [10].

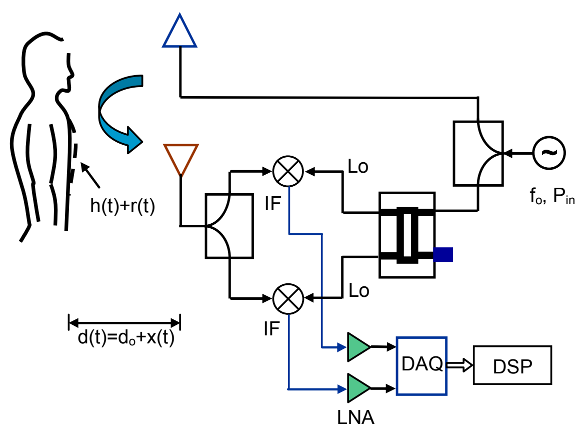

Fig. 1. Schematic block diagram of the Doppler radar system. The in-phase and quadrature components of the baseband signal are captured and processed independently.

The setup deployed in the measurements has separate, but similar, transmitting and receiving antennas to minimize Tx to Rx coupling. Other reported configurations use single antenna and isolate the transmitted and received signals by means of a circulator or a coupler [8]. However, when the two antennas are adjacent and the subject is positioned in the far field, the separation of Tx and Rx antennas has little effect on the measurement results.

Mixing the local oscillator signal with the RF reflected wave results in the baseband signal, which in its quadrature form can be represented as:

$$I_{BB} = A\cos\left[\frac{4\pi \mathrm{f}}{\mathrm{c}}x(t) + \phi_{tot}\right] \tag{1}$$

$$Q_{BB} = A\sin\left[\frac{4\pi \mathrm{f}}{\mathrm{c}}x(t) + \phi_{tot}\right] \tag{2}$$

where, $x(t) = h(t) + r(t)$, is the chest motion composed of heartbeat and respiration, f is the local oscillator frequency, A is amplitude of the complex baseband signal, and ϕ_{tot} is the constant phase due to the fixed roundtrip distance and any initial phase.

On the complex I-Q plot, these equations form an arc that belongs to a circle centered at the origin. The radius of the circle is A, and the angle scanned by the arc corresponds to the time-varying phase in the argument of both the cosine and sine. However, the dc offset mainly caused by clutter reflected signals may shift the center of the circle anywhere in the four quadrants. The dc components of the baseband signals combine the radius A, and the dc offset. Since the received power is proportional to A^2, it is necessary to recover this information to determine the RCS.

The radius A is estimated using the center estimation algorithm implemented in three steps [9]. The role of center estimation algorithm is to find the circle to which the arc belongs and bring the center of the circle to the origin of the complex I-Q plot. The radius of the circle A is the magnitude of the baseband signals and corresponds to the reflected wave power which is proportional to the radar cross section. The radius is obtained by taking the root mean of (I^2+Q^2). First, the algorithm finds the mean of the complex baseband signal and subtracts it from the signal. The mean includes the residual dc offset and almost the entire radius. This brings the arc to the origin of the coordinates. Second, the arc is rotated to be parallel to the y-axis and hence, the center of the circle will be located on the x-axis. Last, the center is obtained knowing that the vector perpendicular to the line joining any two points on the arc passes through the center of the circle. And since the signal is noisy by nature, a statistical median is applied to obtain the estimated center from values calculated for each two successive points on the arc.

In principle, the center estimation algorithm doesn't require cancellation of the dc offset in the baseband signal. However, due to the potentially high dc levels and due to the limited number of bits in the data acquisition system, it is required to minimize the offset to maximize the accuracy by which the ac signals are acquired. In this experiment, the dc offset is minimized by estimating the offset value from the measured signal itself and feeding back this value, with negative polarity, to baseband signal just before the last filtering and amplification stage.

III. RCS CALCULATION

The source signal undergoes several losses of different kinds as it travels to the target and bounces back to the receiver. From the signal generator to radiator, the losses are due to return loss R_{comb} of the 0-degree splitter, the 3-dB splitting, and the antenna return loss R_A. The loss of a 0-dB attenuator in the transmitter path is neglected. The transmitted power P_T is then:

$$P_T = \frac{P_{in}}{2}(1 - R_{comb})(1 - R_A) \tag{3}$$

where, P_{in} is the input power. From transmitting antenna to target and back to receiving antenna, the link budget is governed by Friis formula:

$$P_R = P_T\frac{G^2\sigma_{eff}}{(4\pi)^3 d^4}\left(\frac{c}{f}\right)^2(1 - R_A) \tag{4}$$

where, G is the antennas gain, d is the range and σ_{eff} is the effective radar cross section of the moving surface of the body due to cardiopulmonary activity. This equation is derived is far-field where $d > 2D^2/\lambda$ and D is the largest dimension of the antenna or, in this case, of the moving area of the target.

From receiver antenna to LNA, there is another R_{comb}, 3-dB splitting, mixer return loss R_{mix} and mixer conversion loss L_{conv}. The loss of a BPF connected right after the receiving antenna is neglected. Therefore, the power in baseband is:

$$P_{I/Q} = \frac{P_R}{2}(1 - R_{comb})(1 - R_{mix})L_{conv} \tag{5}$$

The conversion loss of the mixer depends on Lo power. This can be calculated as:

$$P_{Lo} = \frac{P_{in}}{4}(1 - R_{comb})(1\text{-}R_H)(1 - R_{mix}) \tag{6}$$

where, R_H is the return loss of the 90-degree hybrid. Finally the power is converted to a potential difference at the input of the LNA and gets amplified by its gain G_{LNA} according to:

$$A = G_{LNA}\sqrt{2 \times P_{I/Q} \times 50} \tag{7}$$

In this work, P_{in} = 13 dBm, f = 2.4 GHz, G_{LNA} = 5000, d = 1.82 m (6 ft), $G \approx 7$ dB. The return losses are all assumed to be about $(0.2)^2$, corresponding to an SWR of 1.5, and from the ZFM-4212 mixers data sheet, $L_{conv} \approx$ 0.25. The effective RCS will then be $\sigma_{eff} \approx 0.02\, A^2$.

IV. MEASUREMENTS

Two measurements were made on a healthy 30-year-old male subject in lying position. In the first measurement, the subject was lying comfortably on his back (supine). The transmitting and receiving antennas were suspended above the subject at a vertical distance of 1.82 m. The radiating plane of both antennas was parallel to the floor plane. Received signals were recorded while subject was breathing for 90 seconds. In the second measurement, the subject was lying face-down (prone) with the back facing the transceiver antennas. The antennas position was kept the same and again, signals were recorded while subject was breathing for 90 seconds. In each measurement scenario, the quadrature baseband signals were dc-coupled to the LNA's and analyzed using center estimation algorithm with dc cancelation. Two piezoelectric effort belts were used as respiration reference, one for the chest and the other for the abdomen. The subject is 1.65-m tall and weighs 86.1 Kg. In maximum inhale, the subject has a chest breadth of 34 cm and a chest depth of 24 cm. In maximum exhale, the chest breadth and depth are 32 cm and 22 cm, respectively.

V. Analysis and Results

The first 12 seconds of each recorded data correspond to dc estimation and cancellation settling time and can be discarded. The complex data vector of length corresponding to 78 seconds is broken into segments, each corresponds to about a full respiration cycle. In Fig.2, the Fourier analysis of the I-Q data for subject in supine shows a peak at 0.167 Hz. This indicates that one respiration cycle can be rounded to 6 seconds.

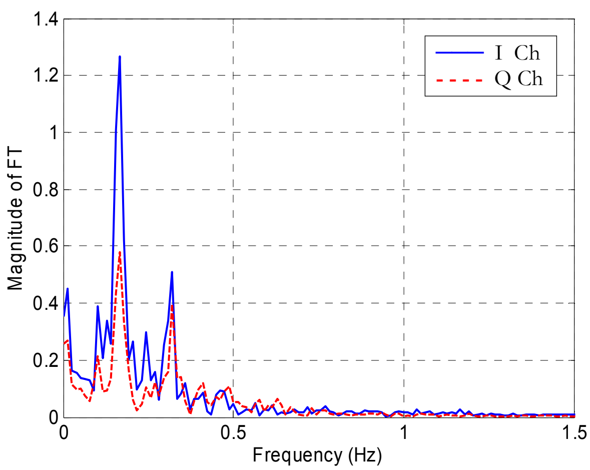

Fig. 2. Fourier transform of quadrature raw channels in case of subject lying on his back. The response is peaked at 0.167 Hz.

The center estimation algorithm is applied to each data segment and the corresponding arc radius is obtained. The result is a vector of length equal to the number of segments. A similar vector is obtained by applying circle fitting algorithm to each segment of data. The amplitude A of the complex baseband signal is determined by examining the mean, the median and the maximum of both amplitudes vectors. The more circular are the segments, the closer all values should be.

The center-tracked arc for subject in supine position is shown in Fig. 3. Only the arc corresponding to one segment of data is displayed. The arc lies on a circle centered at the origin of the coordinates, as expected from the center estimation algorithm. The calculated amplitudes vector using center estimation has a median of 2.58 V, a mean of 2.62 V and a maximum of 4.04 V. From the circle fitting algorithm, the values obtained are 3.82 V, 3.79 V and 4.038 V, respectively. The small difference between the mean and median indicate the amplitude values are evenly distributed around the mean. The matching values of the maxima of both center estimation and circle fitting indicate that the corresponding segment is almost a perfect arc. Since, the mean and median of circle fitting have closer values to the maximum, the latter will be considered to get the RCS. From the loss budget equation and for A = 4.04 V, $\sigma_{eff} \approx 0.326$ m^2.

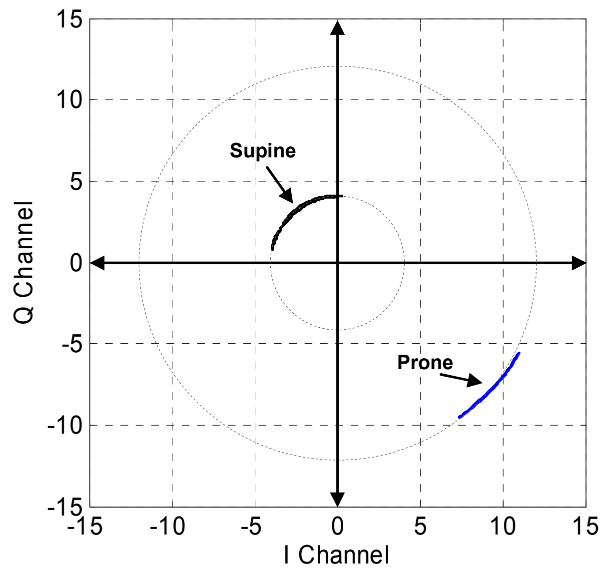

Fig. 3. Center-tracked arcs for subject breathing in 2 lying positions. The estimated circle radius is 4.04 and 12.13 V for body front and back surfaces, respectively.

In the case of subject in prone position, the dc-coupled arc is captured and center-tracked. The latter is also shown in Fig. 3 for one segment of data. The calculated amplitudes vector with center estimation has a mean of 8.05 V, a median of 8.04 V and a maximum of 12.13 V. Whereas the corresponding values using circle fitting are 11.28 V, 11.23 V and 11.86 V, respectively. Again, the values of the amplitudes vector are evenly distributed for both algorithms and the maxima are also comparable. If the maximum is considered as in the previous case, A = 12.13 V corresponds to a an effective RCS of $\sigma_{eff} \approx 2.9$ m^2

Two major differences can be noticed between the cardiopulmonary behavior of a subject in supine and prone positions. First, the arc obtained from the front part of the body in supine scans an angle $\Delta\phi$ larger than the arc obtained from the back in prone, 83.6^o compared to 25.2^o, respectively. The angle represents the modulated phase due to Doppler effect and is proportional to the displacement Δx of the body surface such that $\Delta x = \Delta\phi \times c/(4\pi f)$. Therefore, the displacement of the front body surface is about 1.45 cm while that of the back is 0.44 cm, which is more than three times smaller than the front. This is mainly due to the difference in the nature of motion at the body surface in the two lying positions. When the subject lies on his back, he is breathing almost freely and all motion due to mainly respiration is translated to the front and is manifested in higher latitude. When the subject lies on his front, the motion of the chest and stomach are translated to a uniform motion of the back but with reduced depth due to the weight of the subject, as shown in Fig. 4.

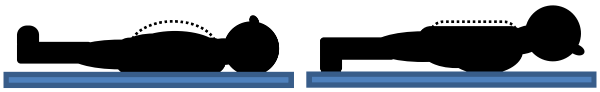

Fig. 4. Motion Characteristics when subject lies in supine and prone positions.

Second, the estimated radius of the center-tracked arc, which corresponds to the complex signal magnitude, is larger when the subject is lying in prone position. In fact, the arc radius obtained from the back of the body is almost three times larger than that obtained from the front. Consequently, the effective RCS of the back is nine times larger that that of the front. This increase in radar cross section is due to the difference in geometrical shapes of the front and back of the body. The front of the body can be modeled as a cylinder with a radius of curvature roughly equal to half the chest breadth, which is around 16 cm for the subject involved in this study. At 2.4 GHz, the wavelength is 12.5 cm, therefore $2\pi a/\lambda = 8$. In terms of region of interaction between the electromagnetic wave and the moving surface of the body, this will be toward the end of the resonance region and close to the optical region. As for the back of the body, the surface is flat enough to be modeled as a sheet with an area roughly equal to the chest breadth squared. According to literature [11], the radar cross section of a flat conducting sheet is larger than that of a cylinder of the same *physical* cross section area, especially in the optical region. This explains the results obtained and suggest modeling the upper part of the body as half a cylinder.

In order to check the far-field condition of the performed measurements, assume the back of the body has a unity reflectivity and that it interacts with the incident wave within the optical region. Therefore, the effective RCS can be expressed as $\sigma_{eff} \approx 4\pi S^2/\lambda^2$, where S is the physical area of the moving part of back body surface. From the calculate RCS of the back of the body, the estimated moving physical area is $S = 0.06$ m^2. For a square, the corresponding diagonal is $D \approx 34.6$ cm. Therefore, $2D^2/\lambda = 1.9$ m, this ensures that $d = 1.82$ m is close enough to the far-filed boundary.

VI. Conclusion

The effective radar cross section of human cardiopulmonary activity is studied for a male subject in supine and prone positions. The radar configuration, system power budget and demodulation algorithm were presented. The RCS of the back of the subject was about nine times as large as the front due to the flatness of the back. On the complex I-Q plot, this is translated to an arc with larger radius of curvature. The radar-determined cross section remains valid as long as the subject respiration and heartbeat motion remains consistent. On the other hand, the arc obtained from the back scanned an angle almost three times smaller than that of the front, indicating that the weight of the body had an effect on reducing the amplitude of the respiration motion. The obtained RCS values suggest modeling the moving part of upper body as a half-cylinder where the front is cylindrical and the back is flat. The radar cross section is expected to further differ for other body orientations. A full understanding of this quantity is a necessary step to enabling extensive quantitative interpretation of cardiopulmonary body motion, subject position, multiple subject separation, and depth of respiration and heartbeat motion.

References

[1] J. Lee and J. Lin, "A microprocessor-based arterial pulse wave analyzer," *IEEE Trans. On Biomedical Engineering*, vol. BME-32, no. 6, June 1985, pp. 451-455.

[2] J. C. Lin, "Microwave sensing of physiological movement and volume change: A review," *Bioelectromagnetics*, vol. 13, pp. 557-565, December, 1992.

[3] B. Lohman, O. Boric-Lubecke, V. M. Lubecke and P. W. Ong, M. M. Sondhi, "A digital signal processor for Doppler radar sensing of vital signs," *IEEE Enginering in Medicine and Biology Magazine*, vol. 21, pp. 161-164, Sept-Oct. 2002.

[4] W. Massagram, N. M. Hafner, B.-K. Park, V. M. Lubecke, A. Host-Madsen and O. Boric-Lubecke, "Feasibility of heart rate variability measurement from quadrature Doppler radar using arctangent demodulation with dc offset compensation," in *Proc. 29th Annu. Conf. IEEE EMBS*, Lyon, France, 2007, pp. 1643–1646.

[5] A. D. Droitcour, T. B. Seto, B.-K. Park, S. Yamada, A. Vergara, C. El-Hourani, T. Shing, A. Yuen, V. M. Lubecke and O. Boric-Lubecke, "Non-contact respiratory rate measurement validation for hospitalized patients," *31st Annu. Conf. IEEE EMBS*, Minneapolis, 2009, to be published.

[6] F. V. Schultz, R. C. Burgener and S. King, "Measurement of the radar cross section of a man," *Proceedings of the IRE*, vol. 46, pp. 476-481, February 1958.

[7] T. Wu, "Radar cross section of arbitrarily shaped bodies of revolution," *Proceedings of the IEEE*, vol. 77, no. 5, pp. 735-740, 1989.

[8] B.-K. Park, A. Vergara, O. Boric-Lubecke, V. M. Lubecke and A. Host-Madsen, "Quadrature demodulation with dc cancellation for a Doppler radar motion detector," submitted to *IEEE MTT Transactions*.

[9] A. Host-Madsen, N. Petrochilos, B.-K. Park, O Boric-Lubecke, V. M. Lubecke, "Optimum demodulation for a Doppler Radar system for vital sign extraction," submitted to *IEEE Signal Processing Letters.*

[10] B.-K. Park, S. Yamada, V. M. Lubecke, and O. Boric-Lubecke, "Single-channel receiver limitations in Doppler radar measurements of periodic motion," *IEEE Radio and Wireless Symp.*, San Diego, CA, USA, pp. 99-102,2006.

[11] M. L. Skolnik, *Introduction to Radar Systems,* 3rd ed., New York: McGraw-Hill Inc., 2001.